

DEPOSITION OF SOLID NANO-COATINGS ON PLASTICS USING ATMOSPHERIC PLASMA

Fernando Alba-Elías

Ana González-Marcos

Jesús Las Heras-Casas

Álvaro Guerra-Sánchez-de-la-Nieta

Departamento de Ingeniería Mecánica. Universidad de La Rioja

Abstract

The systems for the application of solid coatings based on plasma technologies are well known (i.e. CVD ---Chemical Vapor Deposition--- and PVD ---Physical Vapor Deposition---) and their use is pervasive. The solid coatings that are applied improve the functional characteristics of the surface, increasing their hardness or their resistance to corrosion. Most of these technologies use thermal plasma in which the temperature of the surface varies from 200 °C to 1000 °C. This range of temperatures could cause an irreversible phase of thermal softening transformation, or shape changes, in most plastic materials. As an alternative to those methods, this paper will put the focus on the application of solid coatings (SiOx, DLC (Diamond Like Carbon), etc.) structured in shape and size in nanometric scale, using a novel technology based on a source of cold plasma. This deposition technology displays sundry advantages: [1] the temperature of the coating varies from 30 to 80 °C what implies that the integrity of the plastic material to coat is not compromised, [2] the coating is performed on atmospheric pressure what makes possible to install such systems in existing facilities, and [3] it is an innocuous process that does not make use of dissolving substances.

Keywords: *Solid nano-coating; Plastics; Atmospheric plasma*

Resumen

Los sistemas de aplicación de recubrimientos sólidos basados en la tecnología del plasma, son conocidos (p.e. CVD, Chemical Vapour Deposition o el PVD, Physical Vapour Deposition) y su uso está muy extendido. Los recubrimientos sólidos que se aplican, mejoran las características funcionales de una superficie, aumentando su dureza o su resistencia a la corrosión. La mayoría de estas tecnologías emplean plasmas térmicos en los que la temperatura de la superficie varía entre los 200-1000°C. Este rango de temperaturas podría causar una irreversible fase de transformación térmica de ablandamiento, o cambios en su forma, en la mayoría de materiales plásticos. Como alternativa a estos métodos, en esta comunicación se muestra la aplicación de recubrimientos sólidos (SiOx, DLC, etc.) estructurados en tamaño y forma a escala nanométrica (Nano-Recubrimientos Sólidos, NRS), empleando una novedosa tecnología basada en una fuente de plasma "frío" (APCP, Atmospheric Pressure Cold Plasma). Esta tecnología de deposición presentan numerosas ventajas: [1] la temperatura del recubrimiento varía entre los 30-80°C, por lo que no se compromete la integridad del material plástico a recubrir, [2] se realiza a presión atmosférica, por lo que puede instalarse en las líneas de producción existentes, y [3] es un proceso inocuo que no emplea disolventes.

Palabras clave: *Nano-recubrimientos sólidos; Materiales plásticos; Plasma atmosférico*

1. Introduction

EPDM (Ethylene Propylene Diene Monomer) has an elastic behavior, ozone resistance, low weight, favorable mechanical properties, low cost and is easy to fabricate in the desired shapes/and forms. Thus, EPDMs are increasingly used in technological applications as bulk materials. The present work is focused on exploring the deposition of plasma polymer thin films of TEOS (tetraethoxysilane) on an EPDM substrate with a view to improving the characteristics and performance of the elastomer's surface.

Thermal oxidation of silicon and thermal chemical vapor deposition have been well-studied, well-documented, and extensively utilized in both academic and industrial fields to grow silicon oxide (SiO_x) films (Sawada et al, 1996; Raupp et al, 1992), which have become very popular due to their specific chemical structure and protective coating (Yasuda et al, 1997). However, these conventional coating methods do have some limitations or disadvantages (Huang et al, 2009). For instance, the inherently high processing temperatures (typically more than 400° C) of these methods are unsuitable for products that are made of heat-sensitive materials, such as ethylene propylene diene elastomeric monomer (EPDM), which is of interest in this paper.

An alternative method of producing SiO_x films is by low temperature plasma-enhanced chemical vapor deposition. This method is preferred since the deposition temperature can be considerably lower than in other methods (Babayany et al, 1998). However, in spite of their excellent coating efficiency, the currently available coating processes have several major limitations, such as the restricted volume of the plasma reactor and the requirement for one or more vacuum and chemical cycles.

In order to be able to develop industrial types of applications in the future, the atmospheric-pressure plasma jet system (APPJ) (Huang et al, 2009) and the deposition of SiO_x films were chosen. The authors have proposed the use of remote atmospheric pressure plasma deposition because the deposition of a remote APP jet to form SiO_x films on polymeric substrates simultaneously permits the use of a low temperature for coating processing and enables the film structures to be kept relatively constant.

The conformal coverage obtained by plasma-enhanced chemical vapor deposition using tetraethoxysilane (TEOS) is superior to that obtained with silane as the silicon source (6). Thus, TEOS has become the preferred reagent for plasma-enhanced chemical vapor deposition of SiO₂ in many applications.

In the specialized literature (Yasuda et al, 1985; Biederman et al, 1992), it is clear that the deposition rate and quality of the plasma-polymerized film is not only affected by the monomer employed, but also by the process parameters, such as discharge power, monomer flow rate, discharge pressure, and reactor geometry and temperature. For this reason, the present work studies variations in discharge power and deposition speed, considering all other parameters as user--selected.

Previous work of these authors (Alba-Elías et al, 2010) demonstrated a new type of atmospheric pressure plasma deposition process in producing SiO_x coatings on a flexible polymeric substrate. It provided preliminary results for input power variable at various gun speeds. In the present study, a more exhaustive experimental approach is performed, as well as a more structured comparison of different plasma power values in accordance with initial results that were identified in (Alba-Elías et al, 2010). Additionally, morphological analyses are thoroughly examined, including tests based on AFM technology.

This paper reports the details of the processing--structure--property relationship of the deposited TEOS films on EPDM surfaces. The effects of the treatments were investigated by means of scanning electron microscopy (SEM), atomic force microscopy (AFM), Fourier-Transform Infrared with Attenuated Total Reflectance (FTIR-ATR) spectroscopy and X-ray

photoelectron spectroscopy (XPS). The results of these examinations will facilitate a fundamental understanding of the plasma processing parameters for re-engineering an elastomer's surface. This is essential in designing industrial applications as coatings must be produced in controlled and reproducible ways.

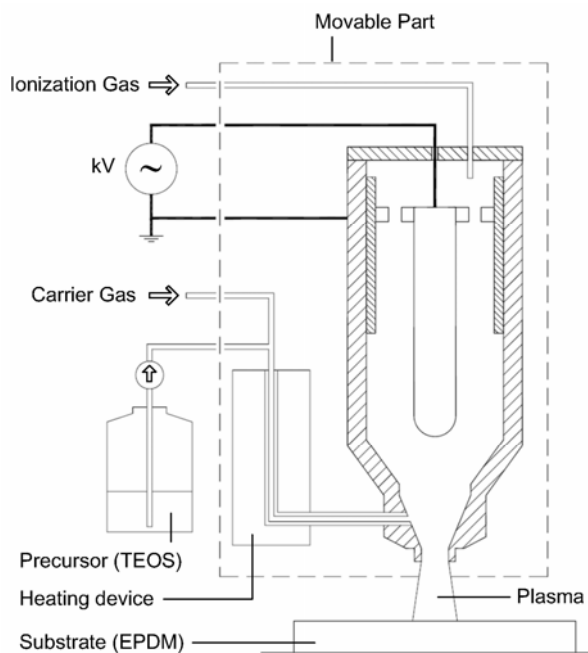
2. Experimental

2.1. Atmospheric pressure plasma deposition system

The plasma glow is ignited by a generator (Plasmatrete, FG5001) with an electrical field applied to the electrodes that are located inside the gun (Plasmatrete, PFW10). An AC power supply of 23 kHz and 15 kV was used.

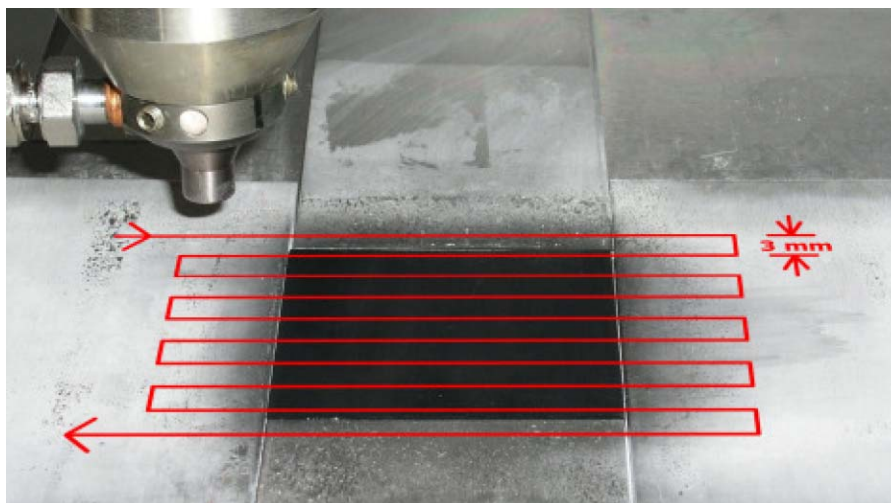
The ionization gas used was Nitrogen (99.99%) with a flow rate of 2000 l/h. It was introduced at the upside of the gun. Nitrogen gas was used also as the carrying gas. It was passed to the precursor system and the flow rate was fixed at 300 l/h. The TEOS monomer was introduced into the mixing system and the temperature was maintained at 180°C. The TEOS flow rate was established at 120 ml/h. The ratio between the vaporized precursor and the carrier gas was 1:2.6. The pressure for applying the precursor gas was fixed at 20 mbar. The distance between the jet and the substrate was maintained at 20 mm.

Figure 1: Schematic jet diagram of the APPJ deposition system



EPDM samples of 50 mm x 50 mm x 2 mm dimensions were used as substrates and cleaned with isopropanol to remove surface contamination before loading into the APPJ system. These samples were fixed between four metal plates (100 mm x 50 mm x 2 mm) in order to facilitate the deposition. As indicated before, different tests were performed by changing operating parameters: a constant deposition speed of 10m/min was used and four different setting of power were analyzed (800, 900, 1000 and 1200 W). For each test, three samples were coated.

Figure 2: Scheme of jet movement across samples



As the samples used are square, the jet is moved across the surface in a scanning movement with a track pitch of 3 mm. The turning points are beyond the metal framing plates (see Fig 2).

2.2. Scanning electron microscopy (SEM)

SEM observations were made using a JEOL JSM-840 scanning electron microscope operating an accelerated voltage of 5 to 30 keV. The non-conducting surface of EPDM and the plasma polymer surfaces were gold coated.

2.3. Atomic Force Microscopy (AFM)

For AFM studies a Veeco Instruments Multimode V with Nanoscope V controller was used. Samples were measured in tapping mode in air using a phosphorus-doped silicon probe (RTESP) delivered by Veeco Instruments. Several scans were performed at different parts of the samples to check the uniformity of the surface. Final images were measured from a scanning area of $10\ \mu\text{m} \times 10\ \mu\text{m}$ with a scanning frequency of 0.5 Hz. No image processing, except flattening, was undertaken. Roughness values were calculated as root-mean-square values (R_q).

2.4. Fourier-Transform Infrared with Attenuated Total Reflectance (FTIR-ATR)

The FTIR-ATR spectra were recorded by use of a BRUKER IFS 66 FTIR spectrometer with a Specac Golden Gate ATR accessory based on a single bounce diamond prism. For every ATR spectrum, 64 scans were taken at a resolution of $2\ \text{cm}^{-1}$.

2.5. X-ray photoelectron spectroscopy (XPS)

X-ray photoelectron spectra (XPS) were acquired by a VG-Microtech Multilab 3000 spectrometer that was equipped with a hemispherical electron analyzer and a $\text{Mg } K\alpha$ ($h\nu = 1253.6\ \text{eV}$, $1\ \text{eV} = 1.6302 \times 10^{-19}\ \text{J}$) 300-W X-ray source. The samples were mounted on a sample rod and transferred to the analysis chamber. Before recording the spectra, the sample was maintained in the analysis chamber until a residual pressure of ca. $5 \times 10^{-7}\ \text{N}\cdot\text{m}^{-2}$ was reached. The spectra were collected at a pass energy of 50 eV. The intensities were

estimated by calculating the integral of each peak, after subtracting the S-shaped background, and fitting the experimental curve to a combination of Lorentzian (30%) and Gaussian (70%) lines. All binding energies (B.E.) were referenced to the C 1s line at 284.6 eV, which provided binding energy values with an accuracy of ± 0.2 eV.

3. Results

3.1. Surface morphology of the coating

The surface morphology of EPDM substrates was observed by SEM and AFM. Figures 3 and 4 show the effect of the input power at a constant deposition speed of 10 m/min on the morphology of plasma-polymerized EPDM substrate. The SEM images are shown at a magnification of x2000 and are representative of the overall surface of the coating (see Fig 3). Regarding the surface roughness (R_q) of the coatings, the average value of the samples for each test was 163.4nm at 800W, 145.1nm at 900W, 115.3nm at 1000W and 111.7 nm at 1200W.

Figure 3: SEM images of coating produced with a deposition speed of 10 m/min with different input power values: (a) 800W, and (b) 1200W.

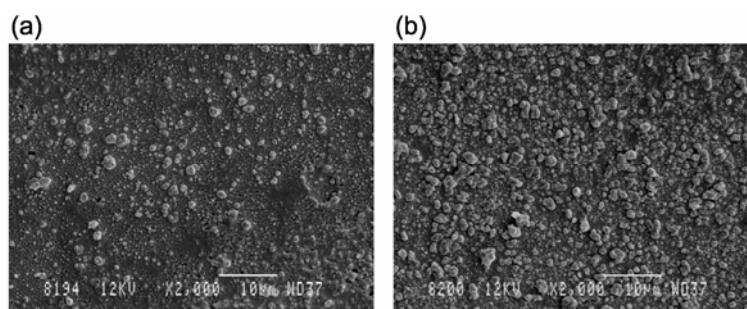
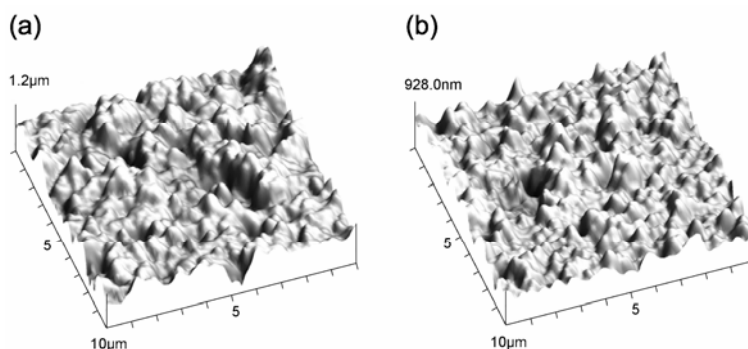


Figure 4: AFM images of coating produced with a deposition speed of 10 m/min with different input power values: (a) 800W, and (b) 1200W.

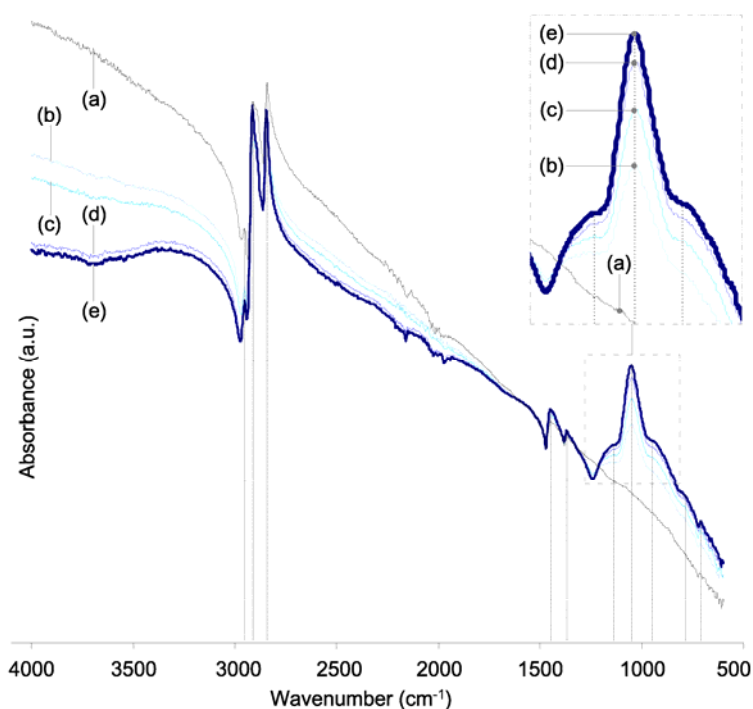


3.2. Chemical structure analysis of the APPJ system

FTIR-ATR was used to characterize the chemical structure and the bonding modes of SiOx layers with variable process parameters. Fig. 5 shows FTIR-ATR spectra of uncoated EPDM and plasma polymerized TEOS coated EPDM at different input power values (800 – 1200W) with a deposition speed of 10 m/min. The uncoated EPDM spectrum (Figure 5a) shows absorption peaks, because of C-H bands, at 2954, 2908 and 2841 cm^{-1} (ethoxy groups) and

1446 and 1365 cm^{-1} (alkyl groups) (Vallee et al, 1997; Jung et al, 2004). All coatings that were prepared (Figure 5b-e) exhibit similar absorption peaks to that of the neat EPDM substrate, indicating that the coating is of sub-micron thickness (Tran, 2005). In addition to the characteristic spectrum for EPDM, four peaks can be identified in the coated samples. The peak at 788 cm^{-1} is attributed to the $\text{SiOCH}_2\text{CH}_3$ group and probably due to incomplete hydrolysis of TEOS (Parry, 2000). It has also been suggested that it originates in symmetric stretching motions of the oxygen atoms (Phanasgaonkar et al, 2009). The peak at 944 cm^{-1} is attributed to Si-OH bending (Yasuda et al, 1997; Hamelmann et al, 2005; Han et al, 2007), a strong absorption band at 1051 cm^{-1} is attributed to Si-O-Si stretching vibrations (Ramamoorthy et al, 2008; Morent et al, 2009; Benitez et al, 2000; Pecora et al, 2006), and a shoulder peak at 1135 cm^{-1} is assigned to the C-O bond of the ethoxy group (Kurosawa et al, 2006). The presence of these groups indicates that the coated samples have a chemical structure that is similar to that of TEOS. The broad band between 3000 and 3600 cm^{-1} is probably due to the presence of Si-OH bonds attributed to O-H stretching (Durrant et al, 2008; Deshmukh et al, 2007; Yin et al, 2009).

Figure 5: FTIR-ATR spectrum of: (a) neat EPDM, and average values of SiOx films obtained at a deposition speed of 10 m/min with different input power values, (b) 800W, (c) 900W, (d) 1000W and (e) 1200 W.



XPS was used to identify the composition and atomic percentages of coatings that were deposited at speeds of 10 m/min, with a monomer flow rate of 2ml/min and various plasma power values (800 - 1200W). The corresponding elemental composition of the coatings and untreated EPDM substrate is given in Table I. For further insight into the chemical bonds present in the plasma-polymerized TEOS films, a curve resolution of the Si2p peak can be undertaken. Table I also shows the proportions of silicon chemical bondings, considering the following binding energies of silicon chemical bonds: SiO_4 at 103.4 eV, CH_3SiO_3 at 102.8 eV, $(\text{CH}_3)_2\text{SiO}_2$ at 102.1 eV, $(\text{CH}_3)_3\text{SiO}$ at 101.5 eV and $(\text{CH}_3)_4\text{Si}$ at 100.9 eV.

Table 1. Average elemental composition of the coatings and untreated EPDM substrate and proportions of silicon chemical bondings.

| Plasma Power (W) | Elemental Composition (at %) | | | Proportions of silicon chemical bondings (at %) | | | | |
|---------------------|---------------------------------|------|------|---|----------------------------------|--|-------------------------------------|------------------------------------|
| | C1s | Si2p | O1s | SiO ₄ | CH ₃ SiO ₃ | (CH ₃) ₂ SiO ₂ | (CH ₃) ₃ SiO | (CH ₃) ₄ Si |
| 800 | 71.8 | 8.1 | 20.1 | 41.1 | 24.3 | 26.6 | 4.6 | 3.4 |
| 900 | 70.0 | 8.3 | 21.7 | 43.2 | 27.7 | 23.4 | 5.4 | 0.3 |
| 1000 | 69.1 | 10.5 | 20.4 | 52.4 | 22.3 | 20.5 | 1.8 | 3 |
| 1200 | 66.5 | 11.2 | 22.3 | 57.6 | 21.0 | 21.4 | 0 | 0 |
| EPDM (uncoated) | 86.3 | 5.3 | 8.3 | - | - | - | - | - |

4. Discussion

The morphological features of the film change significantly with the plasma power of the TEOS deposition: the higher the power of plasma-polymerized coating, the less rough is the surface of the EPDM substrate. The wear resistance of the substrate is well-known to be dependent on the surface morphology. The smoother the surface of the substrate, the better is the wear resistance (Lin et al, 2008).

The main features found in the spectra of plasma polymerized coatings correspond to the Si-O-Si sequence (1051 cm⁻¹). The presence of these vibrational modes is similar to what is seen in the TEOS monomer. It is likely that carbon atoms of the TEOS precursor are incorporated mainly in ethoxy groups (2954, 2908, 2841 cm⁻¹) and alkyl groups (1446, 1365 cm⁻¹) (Vallee et al, 1997; Jung et al, 2004). The broad band between 3000 and 3600 cm⁻¹, associated with OH groups, indicates the presence of bonded water in every film (Benitez et al, 2000). It has been suggested that water incorporated in the film came from water that had accumulated on the layer as a reaction product and then was incorporated into the film and/or water that was taken from the air after treatment (Yasuda et al, 1997; Huang et al, 2009; Jung et al, 2004; Tran et al, 2005; Durrant et al 2008). It is clear that the intensity of peaks of Si-O-Si bonds, ethoxy and alkyl groups, and the plasma power are non-linearly related as the increment rate decreases with the plasma power values. As can be seen in Figure 5, the intensity of the SiOH bonds decreases with the increment of discharge power due to the decomposition of ethyl groups of TEOS. The gas-phase reaction of the precursor decompositions is enhanced by corresponding increases in plasma energy. This leads to an increase in density of the cross-link of the films (Vallee et al, 1997), and a decrease in the intensity of the OH bands (Jung et al, 2004).

In regards to the atomic composition of the coatings, Table I shows that they contain less carbon and more silicon and oxygen than the uncoated EPDM substrate. Furthermore, Table I illustrates how, as the plasma power increases, the atomic percentage of carbon decreases by decomposition of the ethyl groups of TEOS (Jung et al, 2004) and the atomic percentage of silicon and oxygen increases. Finally, an increase in the plasma power results in an increase in the proportion of the SiO₄ chemical bond, as well as a decrease in the proportion of CH₃SiO₃, (CH₃)₂SiO₂, (CH₃)₃SiO and (CH₃)₄Si.

At a high plasma power value, more reactive species of O and Si are created. Then, O reacts with reactive species of Si and more reactive species of Si-O are formed on the surface of the EPDM substrate. This results in a higher proportion of the SiO₄ chemical bond (Table I), which offers an increase in the hardness of the coated surface (Lin et al, 2008).

5. Conclusion

A new type of atmospheric pressure plasma deposition process in producing SiO_x coatings on a flexible polymeric substrate (EPDM) is presented. Specific studies have been performed to explore the effect of different parameters of the plasma-polymerization mechanism on the film's morphological properties. Also, detailed analyses of the bonds between atomic components have been presented in order to facilitate a better understanding of underlying transformations taking place during the atmospheric plasma polymerization processes.

From these studies and analyses, a clear relationship between the plasma power and the morphology of the film was observed. Higher plasma power produces a less rough EPDM substrate. On the other hand, the intensity of Si-O-Si absorbance that is observed in the FTIR-ATR spectra is non-linear related to the plasma power in a positive way. Finally, the hydroxyl groups are negatively related to the plasma power due to moisture in the EPDM substrate. This fact holds true, regardless of the values of the rest of the operating parameters.

In regards to chemical composition, it is noted that the atomic percentage of carbon decreases and the atomic percentages of silicon and oxygen increase as the plasma power increases.

To conclude, the open air procedure (APPJ) that was investigated shows promise as a technique for coating SiO_x layers on polymeric materials, especially when its simplicity and suitability to coat large scale substrates for industrial needs are considered. These films are relevant to industrial applications, due to the different properties fostered, such as protective coating and transmittance (Huang et al, 2009).

Although this work was undertaken to investigate the properties of TEOS films deposited on the EPDM in low temperature, open-air conditions and its chemical properties, it is envisaged that these particular properties will be the subject of study in other interesting research fields.

6. Acknowledgments

This work is made possible thanks to support from CSM Instruments (Switzerland), from the Regional Research Plan of the Autonomous Community of La Rioja (Spain) through the project FOMENTA 2010/02.

7. References

- Alba-Elías, F., Ordieres-Meré, J., González-Marcos, A., Martínez-de-Pisón-Ascacibar, F.J. (2010). *10th International Workshop on non-crystalline solids*.
- Babayany, S.E., Jeongy, J.Y., Tuy, V.J., Parkz, J., Selwynz, G.S., Hicksyx, R.F. (1998). *Plasma Sources Sci. Technol.*, 7, 286-288
- Becker, F.S., Pawlik, D., Anzinger, H., Spitzer, A., J. (1987). *Vac. Sci. Technol. B* 5, 1555
- Benitez, F., Martínez, E., Esteve, J. (2000). *Thin Solid films* 377-378, 109-114

- Biederman, H., Osada, Y. (1992). *Plasma Polymerization Processes*, Elsevier, New York
- Deshmukh, R.R., Shetty, A.R. (2007). *Journal of Applied Polymer Science*, 106, 4075-4082
- Durrant, S.F., Rouxinol, F.P.M., Gelamo, R.V., Trasferetti, C., Davanzo, C.U., Bica de Moraes, M.A. (2008). *Thin Solid Films* 516, 803-806
- Hamelmann, F., Heinzmann, U., Szekeres, A., Kirov, N., Nikolova, T. (2005). *Journal of Optoelectronics and Advanced Materials* 7, 1, 389-392
- Han, Y-H., Taylor, A., Mantle, M.D., Knowles, K.M. (2007). *J. Non-Cryst. Solids* 353, 313-320
- Huang, C., Liu, C-H., Su, C-H., Hsu, W-T., Wu, S-Y. (2009). *Thin Solid Films* 517, 5141-5145
- Jung, S.H., Park, S.M., Park, S.H., Kim, S.D. (2004). *Ind. Eng. Chem. Res.*, 435, 483-5488
- Kurosawa, S., Choi, B-G., Park, J-W., Aizawa, H., Shim, K-B., Yamamoto, K. (2006). *Thin Solid Films* 506-507, 176-179
- Lin, Y.S., Chen C.L. (2008). *Journal of Applied Polymer Science* 110, 2704-2710
- Morent, R., De-Geyter, N., Van-Vlierberghe, S., Dubruel, P., Leys, C., Gengembre, L., Schacht, E., Payen, E. (2009). *Progress in Organic Coatings* 64, 304-310
- Parry, G.C. (2000). *Ph.D. Thesis, Department of Materials Science and Metallurgy, University of Cambridge, Chapter 5.*
- Pecora, A., Maiolo, L., Fortunato, G., Caligiore, C. (2006), *J. Non-Cryst. Solids* 352, 1430-1433
- Phanasgaonkar, A., Raja, V.S. (2009), *Surface & Coatings Technology* 203, 2260-2271
- Ramamoorthy, A., Rahman M., Mooney, D.A., Don MacElroy, J.M., Dowling D.P. (2008). *Surface & Coatings Technology* 202, 4130-4136
- Raupp, G.B., Shemansky, F.A., Cale, T.S. (1992). *J. Vac. Sci. Technol. B*, 10, 2422
- Sawada, Y., Orgawa, S., Kogoma, M. (1995). *J. Phys. D: Appl. Phys.* 28, 1661-1669
- Tran, N.D., Choudhury, N.R., Dutta, N.K. (2005). *Polym. Int.* 54, 513-525
- Vallee, C., Goulet, A., Nicolazo, F., Granier, A. (1997). *J. Non-Cryst. Solids* 216, 48-54
- Yasuda, H. (1985), *Plasma Polymerization*, Academic Press, New York
- Yasuda, N., Takagi, S-I., Toriumi, A. (1997). *Appl. Surf. Sci.* 216, 117-118
- Yin, Y., Liu, D., Li, D., Gu, J., Feng, Z., Niu, J., Benstetter, G., Zhang, S. (2009). *Applied Surface Science* 255, 7708-7712

Correspondencia (Para más información contacte con):

Fernando Alba Elías
Área de Proyectos de Ingeniería. Departamento de Ingeniería Mecánica.
Universidad de La Rioja
C/ Luis de Ulloa 20, 26004 Logroño, La Rioja (España).
Phone: +34 941 299 276
E-mail: fernando.alba@unirioja.es